

Synthesis and mesophase characterization of novel methacrylate based thermotropic liquid crystalline monomers and their polymers†

Cite this: *New J. Chem.*, 2014, **38**, 4357

G. Siva Mohan Reddy,‡*^a T. Narasimhaswamy^b and K. Mohana Raju*^a

A new series of side chain methacrylate monomers with a three phenyl ring core connected by an ester with a terminal alkoxy chain and hexamethylene spacer are synthesized by a multistep synthetic route. The corresponding polymers are realized by free radical solution polymerization. Two structurally similar mesogens are also synthesized for use as models to study the influence of the methacrylic unit on the mesophase characteristics. The molecular structure of the intermediates, monomers as well as the polymers is unambiguously confirmed by Fourier-transform infrared (FT-IR), solution ¹H and ¹³C nuclear magnetic resonance (NMR) spectroscopy and by elemental analysis. The mesophase characteristics of all of the monomers and polymers are determined by hot-stage optical polarized microscopy (HOPM) and differential scanning calorimetry (DSC). These investigations revealed the existence of enantiotropic nematic (N), smectic A (S_A) and smectic C (S_C) mesophases. Furthermore, for a representative monomer and polymer, the presence of the smectic phase is confirmed by variable temperature X-ray diffraction (XRD) where a characteristic layer ordering is noticed. The molecular weight of the polymers is determined by gel permeation chromatography (GPC) and the values are found to be typically in the range of 2.0×10^3 to 3.7×10^3 . The mesogenic polymers are also found to be stable up to 320 °C by thermogravimetric analysis (TGA).

Received (in Montpellier, France)
13th November 2013,
Accepted 22nd May 2014

DOI: 10.1039/c3nj01414b

www.rsc.org/njc

Introduction

Thermotropic side chain liquid crystalline polymers (SCLCPs) were discovered in the 1970s by various research groups.^{1–3} These are usually designed to have a polymeric group as the back bone and a mesogenic core as a side chain. Among the polymer backbones utilized for constructing SCLCPs, acrylic/methacrylic and siloxane units are most popular.^{4–6} Later, side chain liquid crystalline polymers based on the vinyl group also came in to existence.⁷ As far as the side chain core is concerned, mostly two ring systems either with ester, imine or azo links *etc.* are used for constructing SCLCPs.^{8–15} Extensive studies on these polymers examining the influence of the backbone on

the glass transition temperature (T_g) and mesophase temperatures have been reported.¹⁶ For example, the T_g and mesophase transitions have been found to vary from a very low temperature (0 °C) to a high temperature (200 °C) depending on the chemical structure of the polymer backbone.¹⁷ Furthermore, extensive investigations covering the influence of the molecular weight on the mesophase transitions, the evolution of birefringence, differential scanning calorimetry and variable temperature X-ray studies for mesophase corroboration have also been reported on SCLCPs to establish the structure–property correlation.^{18–21}

The development of SCLCPs further paved the way for thermotropic liquid crystalline elastomers (LC elastomers) in which the mesogenic monomers are one of the key components.²² LC elastomers are often prepared by reacting a mesogenic monomer with a non-mesogenic cross-linking agent.^{23,24} However, studies have also shown mesogenic bifunctional monomers serving as cross-linking agents.^{25,26} It is well established from the studies of low molecular weight liquid crystals that the size of the core (aspect ratio) plays a crucial role not only in influencing the mesophase stability but also in determining the nature of the phase.²⁷ Conversely, research involving the variation of core length in liquid crystalline polymers is very limited.^{28,29} In recent years there has been growing interest in methacrylate based side chain liquid crystals as they are key

^a Department of Polymer Science & Technology, Sri Krishnadevaraya University, Anantapur 515003, India. E-mail: smreddy@gmail.com, kmohananaraju2020@gmail.com

^b Polymer Laboratory, CSIR-Central Leather Research Institute, Adyar, Chennai 600 020, India. E-mail: tnsamy99@hotmail.com

† Electronic supplementary information (ESI) available: General procedure for the synthesis of intermediates, monomers and polymers and DSC data of model mesogens. See DOI: 10.1039/c3nj01414b

‡ Current address: Chemical, Metallurgical and Material Engineering, Polymer Technology Division, Tshwane University of Technology, Pretoria, South Africa. ReddySM@tut.co.za.

components for the development of liquid crystalline elastomers which are poised for use as artificial muscles.³⁰ These elastomers are also expected to find application in actuators, membranes and sensors.³¹ Interestingly, the liquid crystalline elastomers make use of three phenyl ring based monomers either as the main component or a cross-linking agent.^{24,25} In view of these current developments, in this work, focus is placed on the incorporation of a three phenyl ring core in the side chain to investigate its influence on the mesophase transition temperatures. Furthermore, to establish the role of a methacrylate back bone on the mesophase characteristics, a three ring model mesogen with a similar core is also examined. The investigation mainly focuses on the synthesis of mesogenic monomers, polymers and model compounds and their mesophase as well as their structural characterization. It should be mentioned that much of the work reported in the literature deals with two phenyl ring based side chain liquid crystal polymers.^{1–6} In contrast to them, SCLCPs with a three ring core show better mesophase stability and as a consequence tolerate non-mesogenic cross-linkers in the preparation of elastomers which are then used for the design of liquid crystal elastomers.^{32–35}

Experimental

Materials

4-Hydroxy methyl benzoate, benzyl bromide, 6-chlorohexanol, 4-ethoxy phenol, 4-butoxy phenol, 4-hexyloxy phenol, 4-benzyloxy phenol, methacrylic anhydride, palladium on charcoal (Pd/C, 10%), *N,N'*-dicyclohexylcarbodiimide (DCC) and *N,N'*-dimethylaminopyridine (DMAP) were purchased from Aldrich, USA and used without further purification. *N,N'*-Dimethylformamide (DMF), tetrahydrofuran (THF), ethanol and methanol were purchased from SD Fine, Mumbai. Dichloromethane (DCM), ethyl acetate, diethyl ether, *n*-hexane, ethyl methyl ketone (MEK), acetone, acetonitrile, isopropanol, 1,4-dioxane, triethylamine, potassium hydroxide (pellets), Celite-540, anhydrous potassium carbonate, anhydrous sodium sulphate, silica gel (100–200 mesh) were obtained from Merck, India and used as received.

Instrumental details

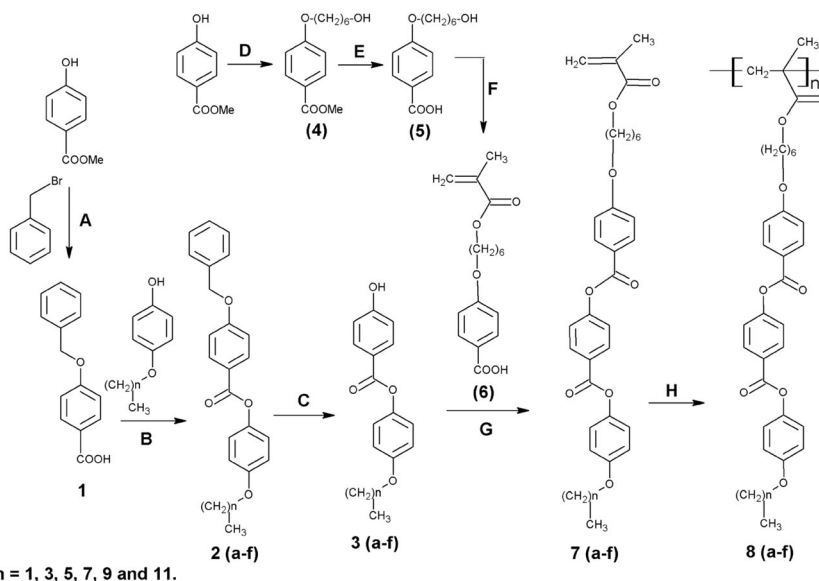
FT-IR spectra of all of the compounds were recorded by an ABB BOMEM MB3000 spectrometer using KBr pellets. ¹H and ¹³C NMR spectra of the compounds in CDCl₃ were run on a JEOL 500 MHz instrument at room temperature using tetramethylsilane as an internal standard. The resonance frequencies of ¹H and ¹³C were 500.15 and 125.76 MHz, respectively. The EI mass spectra were recorded using a JEOL DX-303 spectrometer. Elemental analyses were recorded using an Elemental Analyzer for CHNS, Model-Euro EA 3000, Euro Vector S.P.A. The nature of the mesophase and the temperature of the occurrence of various phases were examined using an Olympus BX50 optical polarizing microscope equipped with a Linkam THMS 600 stage with a TMS 94 temperature controller. The photographs were taken using an Olympus C7070 digital camera. Differential scanning

calorimetry (DSC) traces were recorded on a DSC Q200 instrument with a heating rate of 10 °C per minute in a nitrogen atmosphere. Thermogravimetry analyses of the polymer samples were carried out on a Q-10 series instrument in a nitrogen atmosphere at a heating rate of 10 °C min⁻¹, in the temperature range of 30–800 °C. The weight average and number average molecular weights of the polymers were determined using a WATERS gel permeation chromatograph model BREEZE Million-3 fitted with a DRI detector. Tetrahydrofuran was used as the mobile phase at a flow rate of 1 mL min⁻¹ at 30 °C. The molecular weights were calculated from the calibration curve plotted, using linear polystyrene standards, 1000–60 000. Small-angle X-ray scattering peaks were measured with an evacuated high performance SAXS instrument “SAXSess” (Anton Paar KG, Graz, Austria). The “SAXSess” was attached to a conventional X-ray generator (Philips, Holland) equipped with a sealed X-ray tube (Cu anode target type, producing CuK α X-rays with a wavelength of 0.154 nm), operating at 40 kV and 50 mA. The samples were measured using the paste cell method. The scattered X-ray intensities were detected with a 2D-imaging plate detection system, Cyclone (Packard, A Packard Bioscience Company), with a spatial resolution of 50 × 50 μ m per pixel at a sample to detector distance of 265 mm. Scattering data read from the imaging plate were first corrected for the absorption of the X-rays in the sample and transformed to the *q* scale ($q = 4\pi/\lambda \cdot \sin \theta/2$; program SAXS Quant; Anton Paar KG, Graz, Austria). The SAXS measurements were further corrected with the empty cell measurements.

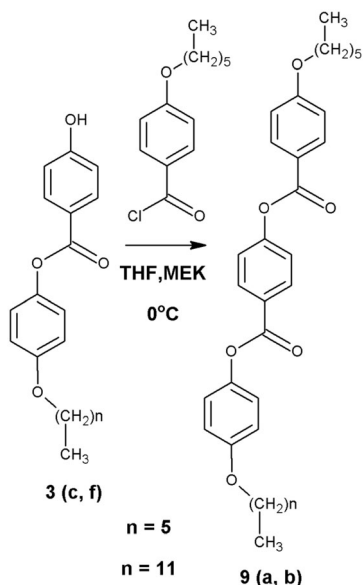
Results and discussion

Synthesis of monomers and polymers

The mesogenic monomers and polymers are synthesized by a multistep strategy as depicted in Scheme 1. The synthetic protocols and the analytical data of the intermediates, model mesogens, monomers and polymers are given in the ESI.† The methacrylate based hexamethylene spacer containing monomers and polymers with a three phenyl ring core and terminal alkoxy groups at one end are synthesized as depicted in Scheme 1. Initially, the 4-hydroxyl methyl benzoate is *O*-alkylated with 6-chlorohexanol in a basic medium. The resulting product (**4**) is hydrolyzed with a base to produce hydroxyhexyloxy benzoic acid (**5**). Upon the reaction of methacrylic anhydride with **5** in the presence of DMAP, the key intermediate (**6**) was produced with a methacrylate unit at one end. Finally, the esterification of the methacrylate intermediate with two ring alkoxy phenols yielded mesogenic monomers **7(a–f)**. The synthesised monomers differ in their terminal chain length and consist of even carbons from C₂–C₁₂. All of the mesogenic monomers are polymerized in solution using benzoyl peroxide as an initiator at 70 ± 1 °C for 24 h under a N₂ atmosphere. The polymers are recovered from their solution in the form of a white precipitate by pouring into excess methanol. The model mesogens, **9(a,b)**, are also prepared without a methacrylic group as per Scheme 2, to examine the influence of the methacrylic group on the mesophase properties.



Scheme 1 Synthetic strategy of the three ring monomers and polymers. (A) DMF, K_2CO_3 , $90\text{ }^\circ\text{C}$; (B) TEA, MEK, $0\text{ }^\circ\text{C}$, 3 h; (C) Pd/C, H_2 , THF, RT, 24 h; (D) $Cl-(CH_2)_6-OH$, DMF, K_2CO_3 , $90\text{ }^\circ\text{C}$; (E) KOH, EtOH, H_2O , reflux; (F) methacrylic anhydride, DMAP, TEA, DCM, $0\text{ }^\circ\text{C}$; (G) DCC, DMAP, DCM/THF, $0\text{ }^\circ\text{C}$, 24 h, and (H) BPO, 1,4-dioxane, $70\text{ }^\circ\text{C}$, 24 h.



Scheme 2 Synthetic strategy of the model mesogens.

Spectral characterization

The FT-IR spectra of a representative monomer and polymer are shown in Fig. 1. The C–H stretching of the aromatic rings at 3071 cm^{-1} and those of the aliphatic units are noticed at 2942 and 2968 cm^{-1} (Fig. 1A). The high intensity absorption peak at 1733 cm^{-1} corresponds to the characteristic C=O stretching of the ester carbonyls in the monomer. The C=C of the methacrylate unit is seen at 1634 cm^{-1} as a low intensity peak whereas the C=C skeletal vibrations of the phenyl rings are noticed at 1604 and 1587 cm^{-1} . The absorptions observed at 1267 , 1244 , 1193 and 1162 cm^{-1} are due to the asymmetric and

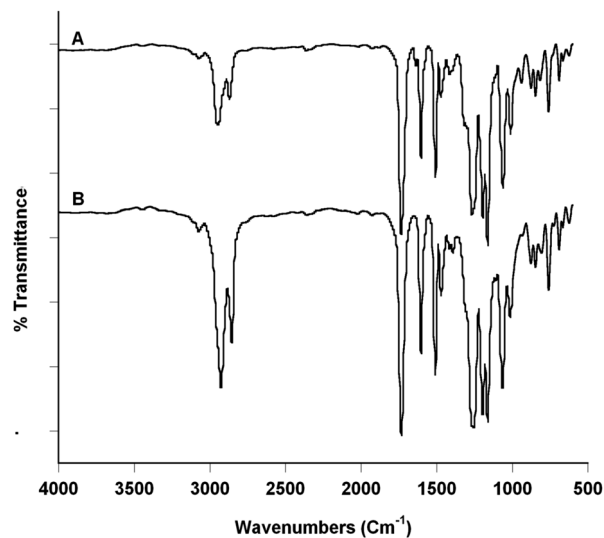


Fig. 1 FT-IR spectrum of (A) monomer **7b** and (B) polymer **8b**.

symmetric C–O–C stretchings of the ether and ester groups present in the monomer. These features are in line with the molecular structure of the monomer. The FT-IR spectrum of the polymer (Fig. 1B), on the other hand, shows similar features to the monomer except the absorption at 1632 cm^{-1} which is due to the C=C bond in the methacrylate unit, a clear indication of the formation of the polymer.

Fig. 2 shows the 1H and ^{13}C NMR spectra of the representative monomer and polymer. The assignment of each signal to the corresponding proton and carbon is carried out by comparing the spectrum with the iterated spectrum obtained using the ACD/chemsketch software, the results are presented in the ESI.† The mesogenic monomer contains four sets of protons arising from

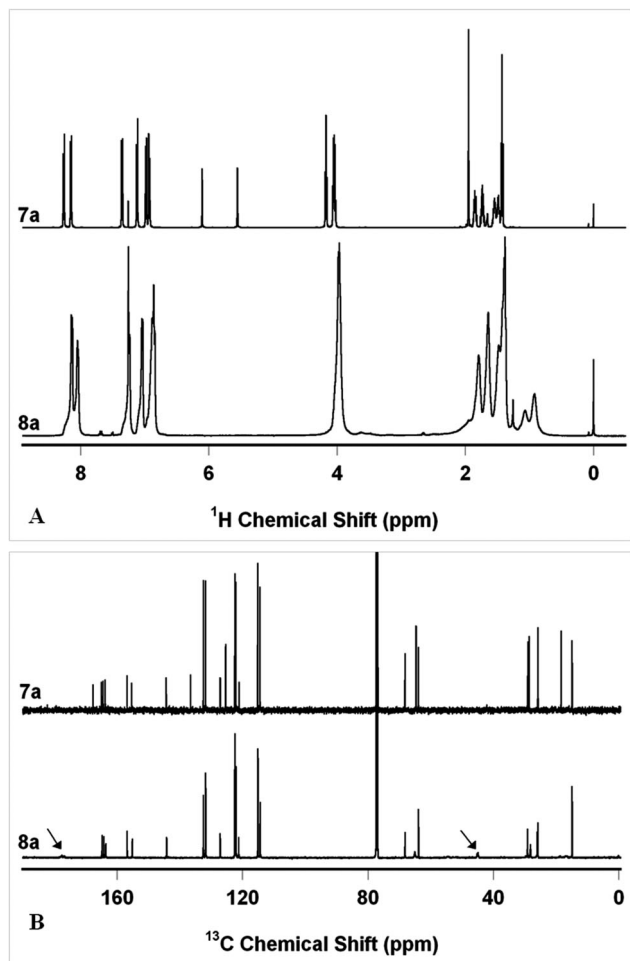


Fig. 2 (A) ^1H NMR spectrum of monomer **7a** and polymer **8a**; (B) ^{13}C NMR spectrum of monomer **7a** and polymer **8a**.

phenyl rings, aliphatic groups including the methyl group of the methacrylate unit, the oxymethylene group and the methylene group of the methacrylate unit, which are clearly identified in the spectrum. Indeed, the ^1H NMR spectrum shows signals in the region of 6.9–8.3 ppm for aromatic protons, 3.9–4.1 ppm for oxymethylene protons, 0.9–2.0 ppm for aliphatic protons and two singlets at 6.1 and 5.4 ppm for the methylene protons of the methacrylate unit. The spectral features such as chemical shift values, multiplicity and peak integrations are very much in line with the structure of the monomer. For the mesogenic polymer, the disappearance of the two singlets at 5.4 and 6.1 ppm associated with the methylene group of the methacrylate unit and the appearance of new signals at 1.8 ppm for a polymeric backbone ($-\text{CH}_2-$) are distinctly seen. Furthermore, the broadening of signals in contrast to the monomer spectrum, owing to the viscous nature of the solution as well as configurational heterogeneity, confirms the formation of the polymer. These trends are also supported by the ^{13}C NMR spectral data and accordingly, the disappearance of two signals for the $\text{C}=\text{C}$ of the methacrylic unit at 125 and 136 ppm and the appearance of a new low intensity signal at 45.9 ppm for the polymeric backbone methylene carbon are observed.

Mesophase transitions by HOPM and DSC investigations

The model mesogens, monomers and their polymers are subjected to HOPM investigation to identify the presence of a mesophase, their transitions as well as the mesophase stability. The results are summarized in Table 1 along with the DSC data. From Table 1, it is evident that all of the synthesized compounds exhibit enantiotropic mesophases. In the case of monomer **7a**, nematic and S_A phases are observed during heating and cooling cycles in HOPM. The sample, on cooling from the isotropic melt, exhibited spherical birefringent droplets and threaded textures (Fig. 3A) which are typical of a nematic phase. Upon further cooling, homeotropic domains with fan textures typical of the S_A (Fig. 3B) phase are noticed. For the monomers **7b**, **7c**, **7d** and **7e**, in addition to nematic and S_A mesophases, a S_C phase is also observed during the cooling cycle (Fig. 3C and D). These mesophases are confirmed by noticing birefringent droplets, focal conic fans and schlieren textures typical of nematic, S_A and S_C phases, respectively. A similar phase sequence is also noticed for monomer **7f** (Fig. 4A–C). Upon continuous cooling of the sample, prior to crystallization, transition bars on the focal conic fans are noticed which are a characteristic of a crystal E phase (Fig. 4D).

The synthesized monomers only differ in their terminal chain length, which varies from C-2 to C-12 carbons (even carbons only). When increasing the terminal chain length of the monomer from C-2 to C-12, a gradual decrease in the isotropic temperature is observed. The nematic, S_A phases are

Table 1 HOPM and DSC data of monomers upon heating

Sample code	Transition observed by DSC	Transition temperature ($^{\circ}\text{C}$)	ΔH (kJ mol^{-1})	Phase observed by HOPM
7a	Cr- S_A	94.0	35.18	Smectic A
	S_A -N	130.0	0.18	Nematic
	N-I	223.0	0.31	Isotropic
7b	Cr- S_C	66.8	42.0	Smectic C
	S_C - S_A	101.0	0.47	Smectic A
	S_A -N	140.0	0.31	Nematic
	N-I	180.0	—	Isotropic
7c	Cr- S_C	72.0	31.8	Smectic C
	S_C - S_A	101.7	0.05	Smectic A
	S_A -N	145.5	0.65	Nematic
	N-I	172.0	1.03	Isotropic
7d	Cr- S_C	69.2	34.8	Smectic C
	S_C - S_A	101.5	0.15	Smectic A
	S_A -N	149.9	1.07	Nematic
	N-I	166.0	0.90	Isotropic
7e	Cr- S_C	61.0	26.58	Smectic C
	S_C - S_A	93.6	0.03	Smectic A
	S_A -N	152.03	1.65	Nematic
	N-I	162.0	0.99	Isotropic
7f	Cr- S_C	63.0	56.05	Smectic C
	S_C - S_A	101.3	0.20	Smectic A
	S_A -N	153.2	4.85	Nematic
	N-I	154.5	—	Isotropic

I: isotropic, N: nematic, S_A : smectic A, S_C : smectic C and Cr: crystallization.

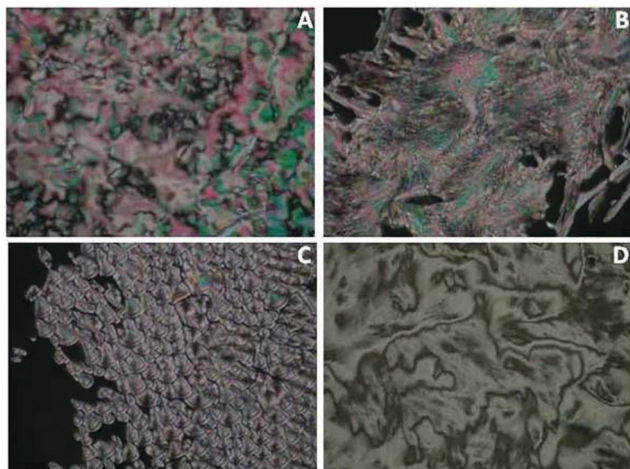


Fig. 3 HOPM photographs of the monomers upon cooling from the isotropic phase (A) threaded nematic phase (**7a**) at 202 °C, (B) smectic A phase (**7a**) at 136.4 °C, (C) transforming to smectic A phase from nematic phase (**7b**) at 142 °C and (D) smectic C phase (**7b**) at 49 °C.

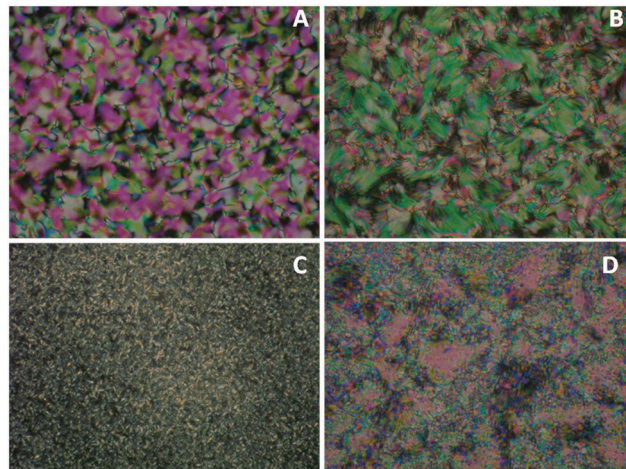


Fig. 5 HOPM photographs of polymers on cooling from the isotropic phase (A) threaded nematic phase of **8a** at 242.3 °C, (B) broken fan texture of smectic C phase of **8a** at 170.5 °C, (C) batonnetts of smectic A phase of **8d** at 220 °C and (D) broken fan texture of smectic C phase of **8d** at 214 °C.

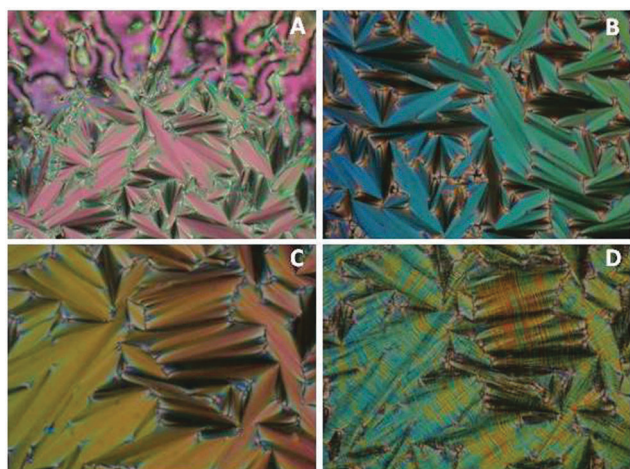


Fig. 4 HOPM photographs of **7f** upon cooling from the isotropic phase (A) transition from nematic to focal conic smectic A at 156.2 °C, (B) focal conic smectic A phase at 154.2 °C, (C) focal conic smectic A phase at 95 °C and (D) crystal E at 30.2 °C.

observed for the ethoxy homologue, for the butoxy homologue, the appearance of a S_C phase is additionally seen. The same trend continues for higher homologues in the series. Interestingly, in contrast to the other homologues, the C-12 exhibited a monotropic crystal E phase. These trends are commonly observed for calamitic mesogens in which the core length is kept constant and the terminal chain length is increased. For the model mesogens (**9a** and **9b**) the appearance of nematic, S_A and S_C phases is also confirmed (table given in the ESI†). In contrast to the model mesogens, the monomer homologues exhibited a drastic decrease in their melting and clearing temperatures with a similar mesophase sequence. This indicates that the incorporation of a methacrylic unit favors a reduction in the melting temperature without affecting the mesophase sequence.

The HOPM examination of the mesogenic polymers also revealed nematic and smectic phases with the variation in the transition temperatures. The mesophase identification is carried out upon cooling the sample from the isotropic melt. During the texture examination, the cover slip of the sandwiched sample is pressed at regular intervals to determine the fluidity. In the cooling cycle, except for the polymer **8b**, crystallization is not observed and instead, the samples showed frozen mesophase textures typical of a glassy nature. In the case of polymer **8a**, **8b** and **8c**, birefringent threaded and broken fan textures are noticed for nematic (Fig. 5A) and S_C (Fig. 5B) phases, respectively. For all of the three cases, the broken fan texture is retained down to room temperature (25 °C). However, upon pressing the cover slips, the fluidity could only be observed over 100 °C and below that it is not noticed. For the polymer **8d**, only S_A and S_C phases are seen in contrast to the lower homologues where the nematic phase is also observed. These polymers also showed batonnetts (Fig. 5C) and broken fan textures (Fig. 5D), these textures are retained even at room temperature. In the case of the polymer **8f**, the disappearance of the S_A phase is observed and it only showed a schlieren and broken fan texture typical of the S_C phase. These observations indicate that improved mesophase stability is noticed for the polymers in contrast to the monomers. Furthermore, the disappearance of the nematic phase for the higher homologues is noted for mesogenic polymers whereas for monomers, the nematic phase is seen even for higher homologues.

The mesophase assignment of monomers and polymers are confirmed by DSC (Fig. 6) where in addition to the transition temperatures, a change in the enthalpy (ΔH) values is also determined. Initially, the DSC experiments of the mesogenic monomers are carried out with a heating rate of 10 °C min⁻¹ (Fig. 6A). This led to broad exothermic peaks in the heating scans suggesting an onset of polymerization owing to the presence of a reactive double bond. Subsequently, the heating

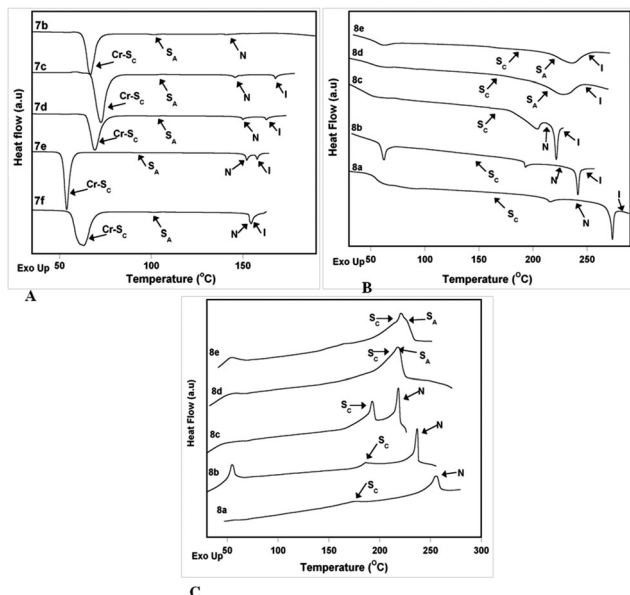


Fig. 6 Differential scanning calorimetry traces of (A) the monomers during a heating cycle (B) the polymers during a heating cycle and (C) the polymers during a cooling cycle.

rate increased to $30\text{ }^{\circ}\text{C min}^{-1}$ to overcome this problem. Hence, the transition temperatures and the associated enthalpy of the 1st heating cycle are considered for the discussion. Table 1 lists the transition temperatures, phase stability and transition enthalpy values of the monomers, determined by the DSC investigation. The appearance of multiple signals in the 1st heating cycle for all of the monomers suggests the occurrence of polymesomorphism which supports the HOPM observations. The transition enthalpy values of the melting temperatures are in the range of $30\text{--}40\text{ kJ mol}^{-1}$, whereas the nematic to isotropic (I) transition value was found to be $\sim 1\text{ kJ mol}^{-1}$. However, for the S_A to S_C transition, a very low enthalpy value is observed indicating a second order transition associated with this phase change.

For the mesogenic polymers which show a glass transition when cooling down from the mesophase, the identification of the phase change is difficult in HOPM. In DSC, on the other hand, it is possible to identify both the first order transition (mesophase transition) as well as the glass transition temperature (second order transition). Accordingly, upon cooling the polymers from the mesophase, glass formation is detected. In the present investigation, the polymers are subjected to DSC (Fig. 6B and C) experiments with a heating rate of $10\text{ }^{\circ}\text{C min}^{-1}$. The data obtained from the 2nd cooling cycle are considered for discussion. Table 2 lists the transition temperatures and the transition enthalpy values obtained from the DSC measurements. It is clear from Table 2 that the enthalpy values of the I–N transitions are $\sim 1.1\text{ kJ mol}^{-1}$ whereas the same values for the I– S_A transitions are found to be $\sim 4.9\text{ kJ mol}^{-1}$. Furthermore, the glass formations in these polymers are found in the range of $42\text{--}54\text{ }^{\circ}\text{C}$.

Powder XRD studies

The powder X-ray diffraction technique is also employed to confirm the existence of smectic mesophases as observed by

Table 2 HOPM and DSC data of the polymers on cooling

Sample code	Transition observed by DSC	Transition temperature ($^{\circ}\text{C}$)	ΔH (kJ mol^{-1})	Phase observed by POM
8a	I–N	255	1.11	Nematic
	N– S_C	175	0.12	Smectic C
	T_g	42	—	Glass transition
8b	I–N	236	1.21	Nematic
	N– S_C	186	0.14	Smectic C
	Cr	54	1.03	Crystallization
8c	I–N	218	1.19	Nematic
	N– S_C	192	0.87	Smectic C
	T_g	54	—	Glass transition
8d	I– S_A	218	4.97	Smectic A
	S_A – S_C	214	—	Smectic C
	T_g	55	—	Glass transition
8e	I– S_A	228	4.87	Smectic A
	S_A – S_C	221	—	Smectic C
	T_g	55	—	Glass transition
8f	I– S_C	225	—	Smectic C
	T_g	54	—	Glass transition

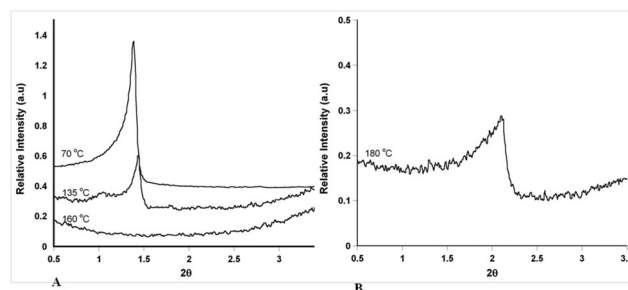


Fig. 7 X-ray diffraction pattern of the (A) monomer **7f** and (B) polymer **8b**.

HOPM and DSC. For a representative mesogen **7f** and polymer **8b**, the diffraction studies are carried out. Fig. 7 shows the diffraction patterns of **7f** as a function of temperature in different mesophases. The spectrum recorded at $40\text{ }^{\circ}\text{C}$ (spectrum not given) showed sharp peaks at small angle and wide angle regions, which confirms the crystalline nature. At $70\text{ }^{\circ}\text{C}$, the diffractogram exhibits a very sharp reflection at $2\theta = 1.39^{\circ}$ and a broad peak at the wide angle region. The disappearance of a large number of peaks and the presence of a very sharp intense reflection at $2\theta = 1.39^{\circ}$ indicates lamellar ordering typical of smectic mesophases.^{36,37} The broad peak at the wide angle region indicates the liquid-like ordering of terminal chains. The spectrum obtained at $135\text{ }^{\circ}\text{C}$ shows a similar diffraction pattern to the spectrum at $70\text{ }^{\circ}\text{C}$ with a small change in the 'd' value. The 'd' value for the $70\text{ }^{\circ}\text{C}$ measurement is 63.48 \AA , whereas for $135\text{ }^{\circ}\text{C}$ the value is found to be 61.27 \AA . Furthermore, the length (L) of the monomer is found to be 44 \AA from the space-filled model. Thus the d/L ratio is ~ 1.4 which indicates the interdigitation of the molecules in the smectic phases.^{38,39} Upon increasing the temperature to $160\text{ }^{\circ}\text{C}$, the disappearance of a small angle sharp reflection is noticed while

the broad peak at a wide angle is intact suggesting an isotropic phase. The XRD scan of the polymer **8b** obtained at 180 °C shows a sharp reflection at the small angle region and a broad hump at the wide angle region similar to **7f**. These features confirm the S_C phase as observed from the HOPM. Thus the XRD data are very much in line with the HOPM and DSC observations.

Thermogravimetric analysis

The thermal stabilities of the synthesized polymers (Fig. 8) are evaluated by thermogravimetric analysis where the samples are subjected to a heating rate of 10 °C min⁻¹. The temperature corresponding to the initial degradation (IDT), 50% decomposition and final degradation (FDT) are listed in Table 3. The IDT temperatures of the polymers are in the range of 320–370 °C, while the typical 50% decomposition is at ~450 °C and the FDT values are in the range of 460–495 °C. Since the structure of the polymer only differs at the terminal chain, the variation in the decomposition temperatures of the polymers is not very high. A comparison of the DSC and TGA data indicates that the clearing temperatures of the polymers are far below the initial decomposition temperature. The observed thermal stabilities of the polymers suggest that the lengthy core with ester connecting units favors high thermal stability.

Gel permeation chromatography

Except polymer **8a**, which is not soluble in THF at room temperature, all of the other polymers are characterized by

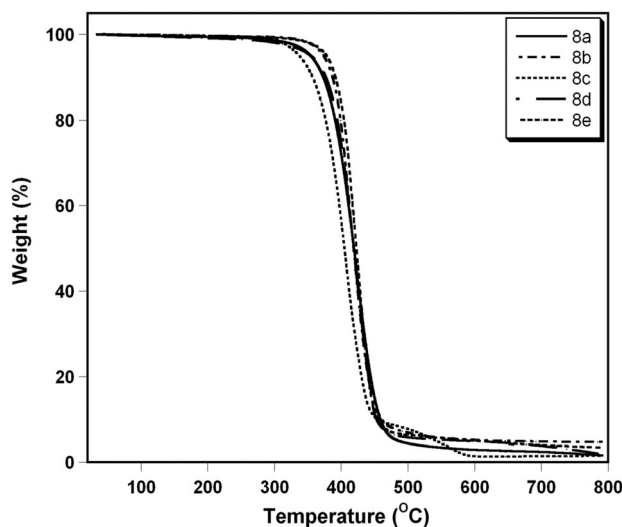


Fig. 8 TGA thermograms of polymers **8a–8e**.

Table 3 TGA data of polymers

Sample code	IDT (°C)	50% DT (°C)	FDT (°C)
8a	339	419	493
8b	359	418	486
8c	319	404	477
8d	355	418	472
8e	369	423	470
8f	354	409	466

Table 4 Molecular weight (g mol⁻¹) and dispersity data of the polymers

Sample code	Weight average molecular weight (M_w)	Number average molecular weight (M_n)	Polydispersity
8b	30 200	16 500	1.83
8c	21 800	12 000	1.81
8d	31 900	18 900	1.68
8e	37 700	22 900	1.64
8f	35 400	22 700	1.55

GPC in order to determine the molecular weight and the dispersity values (Table 4). The weight average molecular weight (M_w) is in the range of 21 800–37 700 g mol⁻¹, while the dispersity index is found to be in the range of 1.55–1.83. This indicates that the three ring monomers are more reactive, due to the presence of the α -methyl group in the backbone. The presence of an electron releasing methyl group in the monomer unit enhances the electron density around the double bond, thereby facilitating efficient polymerization. The dispersity index values obtained are in line with those typically observed for polymers made by free radical initiated polymerization.⁴⁰

Conclusion

A series of methacrylate monomers with three phenyl ring systems, their polymers and their model mesogens are synthesized in order to establish a structure–property relationship. All of the synthesized monomers, polymers and the models exhibited enantiotropic liquid crystalline phases. The polymers with short terminal chains exhibited nematic and smectic phases whereas the increase in terminal chain length resulted in the disappearance of the nematic phase and stabilization of the smectic phases only. An important observation was made with respect to the melting and clearing temperatures where a substantial reduction was noticed after the introduction of a methacrylic unit in the monomer. Interestingly, the mesophase sequence was not altered despite the reduction in the melting and clearing temperatures. The hot stage optical polarized microscopy and differential scanning calorimetry findings were further confirmed by X-ray diffraction studies where layer ordering typical of smectic mesophases was observed. Furthermore, the d/L ratio indicated the interdigitation of molecules in the smectic mesophases. The molecular weights of the polymers were in the range of 2.1×10^3 to 3.7×10^3 . Thermogravimetric analysis revealed that the polymers are thermally stable up to 320 °C and the clearing temperatures are far below the initial degradation temperature.

Acknowledgements

GSMR and TNS sincerely thank Dr A. B. Mandal, Director, CSIR-CLRI for his keen interest and constant support in this work. GSMR also wishes to thank the Department of Science and Technology (India) for financial support, in the form of a fellowship. The authors are also thankful to Dr B. V. N. Phanikumar, CSIR-CLRI, for his help in NMR measurements.

References

- 1 H. Finkelmann, H. Ringsdorf and J. H. Wendorf, *Makromol. Chem.*, 1978, **179**, 273.
- 2 H. Finkelmann, *Polymer Liquid Crystals*, Academic Press, New York, 1982.
- 3 N. A. Plate and V. P. Shibaev, *Makromol. Chem. Suppl.*, 1984, **6**, 3.
- 4 M. Portugall, H. Ringsdorf and R. Zentel, *Makromol. Chem.*, 1982, **183**, 2311.
- 5 G. Rodekirch, J. Riibner, V. Zschuppe, D. Wolf and J. Springer, *Makromol. Chem.*, 1993, **194**, 1125.
- 6 F. Hessel, R. P. Herr and H. Finkelmann, *Makromol. Chem.*, 1987, **18**, 1597.
- 7 J. M. Rodriguez-Parada and V. Percec, *J. Polym. Sci., Part A: Polym. Chem.*, 1986, **2**, 1363.
- 8 L. Xinjuan, F. Liangjing, H. Leigang, Z. Lirong, Z. Ying, Z. Baolong and Z. Huiqi, *Soft Matter*, 2012, **8**, 5532.
- 9 L. Yu, W. Wei and X. Huiming, *Polymer*, 2013, **54**, 6572.
- 10 V. G. K. M. Z. Pisipati, *Z. Naturforsch., A: Phys. Sci.*, 2003, **58**, 661.
- 11 J. H. Liu, P. C. Yang, Y. H. Chiu and Y. Suda, *J. Polym. Sci., Part A: Polym. Chem.*, 2007, **45**, 2026.
- 12 J. H. Liu, Y. K. Wang, C. C. Chen, P. C. Yang, F. M. Hsieh and Y. H. Chiu, *Polymer*, 2008, **49**, 3938.
- 13 G. S. M. Reddy, T. Narasimhaswamy, J. Jayaramudu, E. R. Sadiku, K. M. Raju and S. S. Ray, *Aust. J. Chem.*, 2013, **66**, 667.
- 14 G. C. Andrew, T. I. Rachel, M. F. Alfonso, R. G. Amparo, W. H. Ian and T. I. Corrie, *Eur. Polym. J.*, 2012, **48**, 821.
- 15 L. Wenhan, N. Shusaku and S. Takahiro, *New J. Chem.*, 2009, **33**, 1343.
- 16 C. Noel and P. Navarad, *Prog. Polym. Sci.*, 1991, **16**, 55.
- 17 (a) A. Blumstein and E. C. Hsu, *Liquid Crystalline Order in Polymers*, ed. A. Blumstein, Academic Press, New York, 1978; (b) Q. F. Zhou and X. J. Wang, *Liquid Crystalline Polymers*, World Scientific Publishing, Singapore, 2004.
- 18 S. Esselin, L. Bosio, C. Noel, G. Decobert and J. C. Dubois, *Liq. Cryst.*, 1987, **2**, 505.
- 19 B. Wunderlich, M. Moller, J. Grebowicz and H. Baur, *Adv. Polym. Sci.*, 1988, **87**, 1.
- 20 P. Davidson, *Prog. Polym. Sci.*, 1996, **21**, 893.
- 21 S. Basu, A. Rawas and H. H. Sutherland, *Mol. Cryst. Liq. Cryst.*, 1986, **132**, 23.
- 22 (a) M. Warner and E. M. Terentjev, *Liquid Crystal Elastomers*, Oxford University Press, Oxford, 2003; (b) L. T. de Haan, C. Sánchez-Somolinos, C. M. Bastiaansen, A. P. Schenning and D. J. Broer, *Angew. Chem., Int. Ed.*, 2012, **51**, 12469.
- 23 K. Urayama, *Macromolecules*, 2007, **40**, 2277.
- 24 P. Xie and R. Zhang, *J. Mater. Chem.*, 2005, **15**, 2529.
- 25 B. Donnio, H. Wermter and H. Finkelmann, *Macromolecules*, 2000, **33**, 7724.
- 26 D. J. Broer, G. P. Crawford and S. Zume, *Cross-linked Liquid Crystalline Systems*, CRC, Taylor and Francis Group, Boca Raton, FL, 2011.
- 27 (a) G. W. Gray, *Molecular Structure and the Properties of Liquid crystals*, Academic Press, New York, 1962; (b) G. R. Luckhurst and G. W. Gray, *The Molecular Physics of Liquid Crystals*, Academic Press, New York, 1979.
- 28 C. A. Yang, Q. Tan, G. Q. Zhong, H. L. Xie, H. L. Zhang, E. O. Chen and Q. F. Zhou, *Polymer*, 2010, **51**, 422.
- 29 C. A. Yang, G. Wang, H. L. Xie and H. L. Zhang, *Polymer*, 2010, **51**, 4503.
- 30 M. H. Li and P. Keller, *Philos. Trans. R. Soc. London, Ser. A*, 2006, **364**, 2763.
- 31 (a) W. H. de Jeu and M. Brehmer, *Liquid Crystal Elastomers: Materials and Application*, Advances in polymer science, Springer, Berlin, 2012; (b) C. Ohm, M. Brehmer and R. Zentel, *Adv. Mater.*, 2010, **22**, 3366.
- 32 A. V. Medvedev, E. B. Barmatov, A. S. Medvedev, V. P. Shibaev, S. A. Ivanov, M. Kozlovsky and J. Stumpe, *Macromolecules*, 2005, **38**, 2223.
- 33 O. Kunihiro, M. Yasuyuki, H. Mai and Y. Takashi, *Macromolecules*, 2011, **44**, 5605.
- 34 K. Nobuhiro, N. Takuya, K. Mami, N. Akinobu and K. Mizuho, *Macromolecules*, 2011, **44**, 5736.
- 35 G. Kwak, M. W. Kim, D. H. Park, D. J. Y. Kong, S. H. Hyun and W. S. Kim, *J. Polym. Sci., Part A: Polym. Chem.*, 2008, **46**, 5371.
- 36 (a) A. De Vries, *Mol. Cryst. Liq. Cryst.*, 1985, **131**, 125; (b) A. Shanavas, T. Narasimhaswamy and A. S. Nasar, *Aust. J. Chem.*, 2012, **65**, 1426; (c) M. Kesava Reddy, K. Subramanyam Reddy, K. Yoga, M. Prakash, T. Narasimhaswamy, A. B. Mandal, N. P. Lobo, K. V. Ramanathan, D. S. Shankar Rao and S. Krishna Prasad, *J. Phys. Chem. B*, 2013, **117**, 5718.
- 37 (a) F. Hardouin, A. M. Levelut, M. F. Achard and G. J. Sigaud, *J. Chim. Phys. Phys.-Chim. Biol.*, 1983, **80**, 53; (b) V. N. Raja, D. S. Shankar Rao and S. Krishna Prasad, *Phys. Rev. A: At., Mol., Opt. Phys.*, 1992, **46**, 726.
- 38 G. W. Gray and J. W. Goodby, *Smectic Liquid Crystals*, Heyden, Philadelphia, 1984, p. 134.
- 39 A. M. Levelut, R. J. Tarnto, F. Hardouin, M. F. Achard and G. Sigaud, *Phys. Rev. A: At., Mol., Opt. Phys.*, 1981, **24**, 2180.
- 40 J. E. Mark, *Polymer Data Handbook*, Oxford University Press, New York, 2nd edn, 1999.